ANALYSIS OF THE PRIMARY CONTAINMENT RESPONSE USING A HYDRODYNAMIC ELASTIC-PLASTIC COMPUTER CODE

Y.W. CHANG, J. GVILDYS, S.H. FISTEDIS

Engineering Mechanics Section, Reactor Analysis and Safety Division, Argonne National Laboratory, Argonne, Illinois 60439, U.S.A.

SUMMARY

The dynamic response of the primary containment to a hypothetical core disruptive accident (HCDA) is determined from the basic equations of mass, momentum and energy, and the equations of state of the medium. These equations are first expressed in material coordinates and then set into finite-difference form and solved numerically on the computer. Propagation of pressure waves, loads imposed on different parts of the reactor components, and the resulting deformations are determined at every time step throughout the sequence of the calculation.

Media inside the reactor containment are treated as hydro-elastic-plastic materials. The yield condition of von Mises is used to describe the elastic limit, where for fluids, the yield strength is set to zero. Shell equations are used to determine the dynamic response of the reactor vessel in which the vessel material is considered to be elastic-plastic, strain-hardening, and strain-rate sensitive, where incremental strain theory of plasticity is used. The thickness of the shell is idealized by layers of sub-shells that can carry only normal stresses in the planes parallel to the tangential plane of the shell surface. These sub-shells are connected by the material which carries only shears. The strain-hardening solid is represented by a model in which the thickness of the sub-shell is further decomposed into subregions of elastic-perfectly-plastic materials having different yield stresses, but common strains. Nonphysical numerical oscillation is prevented by the use of the artificial viscosity, whereas the mesh distortion is regularized by a mesh stabilization scheme.

A sample calculation is presented. The mathematical model is discussed, particularly in the areas of modeling of reactor internals. The computer results are presented in both the numerical and pictorial form. Of particular interest are the computer-generated reactor configurations at various times during the excursion. These configurations show the sequence of events which had taken place during the excursion. They show (1) how the deformation of the core barrel, vessel wall, and other structures adjacent to the core become progressively larger with time, (2) how the coolant slug is being pushed upward until it comes in contact with the reactor cover, (3) how the deformation at the upper vessel occurs during the slug impact, and (4) how the vessel regains its equilibrium after the slug impact. Also of interest is the partition of energy which is shown as a function of time. It shows how the core disruptive energy is transformed into other forms of energy. A proper understanding of the energy partition should enable reactor designers to produce better system and containment designs.

1. Introduction

Although large liquid metal fast breeder reactors (LMFBR) can be designed for safe and reliable operation, and the occurrence of a whole core meltdown accident has an extremely low-probability, the safety assessment of the reactor design requires an analysis on the capability of the primary containment system to sustain the consequences of such an accident, even though it is a hypothetical one. In the USA the safety criteria require that the primary containment should not be breached throughout the event, the decay heat must be continuously removed from the damaged core without causing a melt-through of the primary containment, and the fission products and other harmful radioactive materials should be prevented from release to the surrounding environs.

To accomplish this objective, the reactor designer must know the amount of energy released in such an accident, and the energy available for performing work on the system. A major part of the fast reactor safety work in the U.S. has been concerned with estimates of these energies. Methods and calculations of this nature have been in progress for several years. However, the final objective of most accident analyses is to determine what effect the excursion will ultimately have on the primary containment; therefore, the reactor designer must also know the dynamic response of the reactor system to accident loads.

The determination of the dynamic response of the primary system to a hypothetical nuclear excursion is a complex problem. It involves not only the calculation of the response of containment structures, but also the propagation of shock waves, the interactions of fluid and structures, the loads imposed on components and structures adjacent to the core, and the damage produced by these loads. The reactor designer must also know the sequence of failure of the various components, since early failure of one component may change the loadings on other parts of the system.

Because of the complexity of the problems, the early approach was to perform model experiments, in which the hypothetical core disruptive accident (HCDA) was simulated by chemical explosives and the sodium coolant was replaced by water. Although these experiments gave detailed results, their application was limited. Not only the reactor containment structure and internals must be properly represented by a scaled model, but also the rate of energy release from the core must be comparable to that of the chemical explosive. If the reactor system configuration and/or the magnitude and duration of energy release does not fall within the spectrum that has been studied experimentally, judicious estimates must be made in applying the results of the experiments. Quite often the experimental results are incorrectly or unreliably interpreted.

A different approach to the problem is to use the basic conservation equations of mass, momentum, and energy, together with the equations of state of the reactor materials, and calculate the response of containment structure under postulated nuclear excursion conditions. In recent years, the development of high-speed computers has made it feasible to use computer codes to solve numerically the conservation and state equations and to determine the loadings, strains, and the response of the primary containment during the excursion. By use of the appropriate constitutive relations for structural components, the deformation and response of these internal components can also be included in the calculation.

This approach has been used by Argonne National Laboratory in developing the Reactor Excursion Containment Codes (REXCO) [1]. The hydrodynamic version of the REXCO code (REXCO-H) has been described in detail in references [2 - 4]. This paper describes the

hydrodynamic-elastic-plastic version of the REXCO code (REXCO-HEP), which treats not only the hydrodynamics, but also the elastic-plastic deformation of the reactor structures. In addition, recent improvements and developments in the REXCO code will be discussed. As a sample calculation, the code is applied to analyze the response of the FTR reactor to a 150 Mw-sec HCDA. The mathematical model will be discussed, particularly in the areas of modeling of reactor internals, and extending the time range for which reliable calculations can be made.

2. Description of the Hydrodynamic-elastic-plastic REXCO Code (REXCO-HEP)

2.1 Basic Equations

2.1.1 Governing Equations for Elastic-plastic Materials

Solid materials inside the reactor containment are treated as elastic-plastic materials. In this paper, we consider only the case of a cylindrical reactor with axial symmetry; that is, there is no motion in the circumferential θ direction and no variables of the system depend upon θ. Let the distance along the axis of symmetry be denoted by z, and let r denote the radial distance. Denote the Lagrangian coordinates by R and Z and define the Lagrangian coordinates to be the position of the material at t = 0. The actual position r and z of the materials at a later time are dependent variables. They are functions of (R, Z, t). The other variables, density, pressure, etc. are all functions of (R, Z, t). The momentum equations are

$$\begin{aligned} \ddot{r} &= \frac{1}{\rho}\left[-\frac{\partial(P-s_{rr})}{\partial r}+\frac{\partial \sigma_{rz}}{\partial z}+\frac{s_{rr}-s_{\theta\theta}}{r}\right] \\ \ddot{z} &= \frac{1}{\rho}\left[-\frac{\partial(P-s_{zz})}{\partial z}+\frac{\partial \sigma_{rz}}{\partial r}+\frac{\sigma_{rz}}{r}\right] \end{aligned} \tag{1}$$

where ρ is the density, $P = p + q$, with p the mean pressure and q the pseudoviscous pressure, s_{rr}, $s_{\theta\theta}$ and s_{zz} are the deviatoric component of the radial, circumferential and axial stresses, respectively, σ_{rz} is the shearing stress, and the $(\cdot)$ denotes time differentiation along the particle path.

The energy equation is

$$\dot{E} = -P\dot{V} + V(s_{rr}\dot{e}_{rr} + s_{zz}\dot{e}_{zz} + s_{\theta\theta}\dot{e}_{\theta\theta} + \sigma_{rz}\dot{e}_{rz}) \tag{2}$$

where $\dot{e}_{rr}$, $\dot{e}_{zz}$ and $\dot{e}_{\theta\theta}$ are the strain rate components.

They are defined as

$$\begin{aligned} \dot{e}_{rr} &= \frac{\partial \dot{r}}{\partial r} \\ \dot{e}_{zz} &= \frac{\partial \dot{z}}{\partial z} \\ \dot{e}_{\theta\theta} &= \frac{\dot{r}}{r} \\ \dot{e}_{rz} &= \frac{\partial \dot{z}}{\partial r}+\frac{\partial \dot{r}}{\partial z} \end{aligned} \tag{3}$$

The conservation of mass can be stated very simply in terms of strain rate components, as

$$\rho^{-1}\dot{\rho} = -(\dot{e}_{rr} + \dot{e}_{\theta\theta} + \dot{e}_{zz}) \tag{4}$$

or $$\frac{\dot{V}}{V} = \frac{\partial \dot{r}}{\partial r}+\frac{\partial \dot{z}}{\partial z}+\frac{\dot{r}}{r}$$

In a Lagrangian formulation, volume elements are defined by material points, so that mass is conserved implicitly.

The equation of state allows the strain increments calculated in eq. (3) to be converted into stresses. For elastic-plastic materials, the stress rate components, up to the elastic limit, are calculated from

$$\begin{aligned}
\dot{s}_{rr} &= 2\mu\left(\dot{e}_{rr} - \frac{1}{3}\frac{\dot{V}}{V}\right) + \delta_{rr} \\
\dot{s}_{zz} &= 2\mu\left(\dot{e}_{zz} - \frac{1}{3}\frac{\dot{V}}{V}\right) + \delta_{zz} \\
\dot{s}_{\theta\theta} &= 2\mu\left(\dot{e}_{\theta\theta} - \frac{1}{3}\frac{\dot{V}}{V}\right) \\
\dot{\sigma}_{rz} &= \mu\left(\dot{e}_{rz}\right) + \delta_{rz}
\end{aligned} \tag{5}$$

where μ is the shear modulus, and δ_{rr}, δ_{zz} and δ_{rz} are the correction factors for rotation. For stresses beyond the elastic limit, the von Mises yield criterion is employed, namely

$$s_{rr}^{\ 2} + s_{zz}^{\ 2} + s_{\theta\theta}^{\ 2} + 2\sigma_{rz}^{\ 2} - \frac{2}{3}\left(\sigma_o\right)^2 = 0 \tag{6}$$

where σ_o is the yield stress of the given material under uniaxial stress conditions.

2.1.2 Governing Equations for Fluids

Fluids are assumed to be compressible but non-viscous. The conservation equations become

$$\begin{aligned}
\ddot{r} &= -\frac{1}{\rho}\frac{\partial P}{\partial r} \\
\ddot{z} &= -\frac{1}{\rho}\frac{\partial P}{\partial z} \\
dE &= -PdV \\
\frac{\dot{V}}{V} &= \frac{\partial \dot{r}}{\partial r} + \frac{\partial \dot{z}}{\partial z} + \frac{\dot{r}}{r}
\end{aligned} \tag{7}$$

The equation of state is assumed to have the form

$$p = f(V,E) \tag{8}$$

If the value of σ_o in eq. (6) is set equal to zero, the stress deviators will be equal to zero automatically, and eqs. (1) and (2) will reduce to the governing equations for fluids.

2.1.3 Governing Equations for Shell Structures

In an LMFBR, the reactor vessel is normally made of thin steel shells. If the reactor vessel is to be treated as an elastic-plastic solid material, the thickness of the vessel wall will have to be divided up into at least 3 or 4 Lagrangian zones. Large numbers of Lagrangian meshes will be used in the numerical analysis, even for a simple configuration. Therefore, as an option in the REXCO-HEP code, the reactor vessel can be analyzed as thin shell structures.

The equations of equilibrium for a shell of revolution undergoing large deflections are

$$\frac{\partial}{\partial s}\left[N_\phi r\cos\phi\right] - \frac{\partial}{\partial s}\left[Q_\phi r\sin\phi\right] - N_\theta + pr\sin\phi - m\ddot{r}r = 0$$

$$\frac{\partial}{\partial s}\left[N_\phi r\sin\phi\right] + \frac{\partial}{\partial s}\left[Q_\phi r\cos\phi\right] - pr\cos\phi - m\ddot{r}z = 0 \qquad (9)$$

$$\frac{\partial}{\partial s}\left[M_\phi r\right] - M_\theta\cos\phi - Q_\phi r = 0 \quad ,$$

where s is the length of the shell along the meridian, measured from the vertex of the shell, m is the mass of the shell per unit area, ϕ is the angle of inclination of the element with respect to the r-direction, p is the pressure, N_ϕ and N_θ are two tangential stress resultants, Q_ϕ is the transverse stress resultant, and M_ϕ and M_θ are the two stress couples. The thickness of the shell is idealized by layers of sub-shells that can carry only normal stresses in the planes parallel to the tangential plane of the shell structure. These sub-shells are connected by the material which carries only shears. The vessel material is considered to be elastic-plastic, strain-hardening, and strain-rate sensitive. The strain-hardening shell is represented by a model in which the thickness of the sub-shell is further decomposed into subregions of elastic-perfectly-plastic materials having different yield stresses, but common strains. The von Mises yield condition and the incremental strain theory of plasticity are used.

2.2 Equation of State of the Media

As stated in the previous section, the solution of the conservation equations requires an equation of state of the form given in eq. (8). Unfortunately, our knowledge about the equations of state of the reactor materials, particularly in the reactor core and under high temperature conditions is very limited. There exists a wide diversity of opinion about the best way to approximate this information. As a result, it is not possible to provide in the REXCO-HEP a single general form of the equation of state that would be useful and acceptable to all materials. Therefore, different forms of equations of state have been built in the REXCO-HEP code. They are:

(a) MARS equation for vaporizing core (APDA-198)

$$p = A\exp\left(-\frac{B}{T + T_o} + C\right)$$

(b) Pressure as a function of volume $\left(\frac{V}{V_o}\right)$ in tabulated form

$$p = f\left(\frac{V}{V_o}\right)$$

(c) Two-phase equation for oxide core (BNWL-760 Supplement UC-80)

$$p_V = \exp(A + \frac{B}{T} - C\log_e T)$$

$$p_\ell = \left(\frac{\partial p}{\partial T}\right)_\rho (T - T_d) + p_d$$

(d) Mie-Grüneisen

$$p = p_H + \frac{\gamma}{V}(E - E_H)$$

(e) Murnaghan

$$p = \frac{B_o}{B'_o}\left[\left(\frac{V_o}{V}\right)^{B'_o} - 1\right]$$

(f) Ideal gas

$$p = \frac{(\eta - 1)E}{V}$$

(g) TNT explosives

$$p = \frac{E}{\beta V} + \alpha\left(\frac{1}{V}\right)^{\gamma}\left[1 - \frac{1}{\beta(\gamma - 1)}\right]$$

Equations related to fuel-coolant interaction which have been used in the REXCO-HT, an augmented version of REXCO-H, for heat transfer calculations, have not been included in the REXCO-HEP code.

2.3 Numerical Technique

In the numerical analysis, all equations are first expressed in material coordinates and then set into numerical form by finite-difference equations. Shock discontinuities and other numerical oscillations are eliminated by the use of artificial viscosities. The numerical solution of these finite-difference equations is done on the IBM-360 Model-195 computer.

For each problem, the code computes the accelerations, velocities, displacements, change of volumes, densities, strains, pressures and specific energies at every spatial point for a specific time interval. For elastic-plastic materials, the code calculates also the deviatoric stresses and distortion energies. These computations are repeated for every time interval until the maximum time specified is reached, reactor vessel ruptures, or the force acting on the vessel head exceeds the strength of the vessel holddown bolts, whereupon the computation ceases. Figure 1 is a flow chart of the REXCO-HEP code.

2.4 Artificial Viscosity (q)

Artificial viscosity was first introduced by von Neumann and Richtmyer [5] to permit numerical calculations of shock hydrodynamics by replacing the discontinuous pressure jump across a shock by a rapid but continuous change. This device has been proven to be very useful also in preventing oscillatory solutions in the numerical computations. Four types of q are available in the REXCO-HEP code. They are linear, quadratic, Navier-Stokes, and rotational q.

2.5 Mesh Regularization

The disadvantage of using the Lagrangian codes is the limitation imposed on the distortions of the Lagrangian zone. In some problems, particularly in the case of low-energy excursions, the zone distortions may increase and become extreme when the calculations are being extended to cover the entire excursion phenomenon. Therefore, it is necessary to have some means to eliminate or minimize the zone distortions so that reliable calculations can be obtained when the computation time is being extended.

Recent studies [6,7,8] reveal that some severe distortions of the Lagrangian zones are not physically real. They are caused by the method of solution, rather than the physics of the problem. One of the most frequently occurring non-physically-real distortion is the

"hour-glass" distortion of a quadrilateral mesh. The zone sides of the quadrilateral increase and decrease alternately in such a way that the volume of the mesh remains uncharged; therefore, no restoring force is introduced. Once this mode of distortion starts, it will keep growing until the numerical computations become unstable. Therefore, for this type of zone distortions, it is perfectly justifiable to introduce a scheme to control or regulate these non-physically-real distortions.

LASL developed a mesh regularizing scheme [6] for incompressible flows. They introduced a damping force which tends to keep a mesh vertex in the center of mass of its eight adjacent neighboring vertices. Hoskin [9] has incorporated the LASL's scheme into a compressible Lagrangian code, ASTARTE. A different mesh regularization scheme is used in the REXCO-HEP, which utilizes an artificial rotational force to prevent the non-physical distortions from growing. The magnitude of the rotational force is proportional to the rate of the relative rotation of the opposite zone sides. This scheme has been tested successfully on many problems. It can reduce and minimize the zone distortions in the numerical calculations and thus extends the calculations to much longer times.

2.6. Comparison with Experimental Excursion Data

ANL has compared experimental excursion data with REXCO computations [10,11,12,13]. The results of the comparisons have demonstrated that the structural response to a chemical high-explosive charge, as well as slug impact loading, can be predicted by the computer code. The question remaining to be answered is how well the code will predict the response to a hypothetical core disruptive accident postulated for an LMFBR, since the energy release in an HCDA is quite different from that of a high-explosive. To further verify the validity of the REXCO code in this area of postulated accidents, REXCO was used to predict the test results of a 1/30th-scale FTR complex model test performed by SRI [14].

Comparison of the pre-test predictions with the test results was quite favorable. Although it was not possible to compare all data, several of the more important points matched well. For example, in the test the slug arrival time at the vessel head was 1.56 msec. The code calculation showed the start of the head contact at 1.3 msec, which completed head impact at about 1.6 msec. Maximum vessel strains were noted in both the test and calculations occurring at the same location. At the vessel top, a hoop strain of 2.1 percent was found in the experiment, while the calculated strain was about 2.2 percent. At the core midplane, the maximum strain measured was 1.25 percent and the calculated was a somewhat conservative 1.9 percent. The calculated deformation modes were also matched with the experimental results. It demonstrates that the REXCO code can be applied with confidence to compute the consequences of an HCDA if provided with an initial distribution of energy in the core and with accurate equations of state for the core and surrounding structures.

Recently, the REXCO-HEP code was used to determine the gas characteristics of a shock-free energy source [15] developed by Stanford Research Institute for use in scaled model tests to simulate the gas work of a sodium-vapor explosion. The experiments were evaluated by comparison of observed data with REXCO analysis [16]. The gas characteristics were defined in terms of the pressure-volume relation. This relation was then applied in the REXCO-HEP code to simulate experiments and to compute the gas pressure and piston displacements as a function of time. Agreement of computed and measured data is remarkably good.

3. Sample Problem

3.1 Mathematical Model

The FTR reactor shown in Fig. 2 is used as a sample problem for the REXCO-HEP analysis. As can be seen from Fig. 2, the FTR reactor is very complex. No computer code, no matter how sophisticated, can include all the details of the reactor in the mathematical model. Furthermore, it is also impractical to produce a mathematical model that will have the same complexity as the FTR reactor. Therefore, to perform a manageable computer analysis, the representation of the FTR reactor must be simplified.

The important question is to what degree the representation of the FTR reactor can be simplified, so that (1) reliable analysis of the model is still achieved by the computer code, (2) the results are on the conservative side, but are not too over-conservative, and (3) the model accurately describes the response of the FTR reactor under the HCDA loads.

The general approach to the mathematical model is to incorporate, to the extent possible, the correct material properties and equations of state of the reactor materials, especially for critical materials such as the vessel and core barrel. Fig. 3 shows the mathematical model used in the REXCO analysis. Features included are (1) the vessel and thermal liner, including the vessel support ring, head flange and ellipsoidal bottom, (2) the core support structure, (3) the core barrel, (4) the radial and axial shields, (5) the radial and axial reflectors, (6) the fission-gas plenum, (7) the core, and (8) the shield plug and holddown bolts. Several of the internal details such as the instrument trees (IV), in-vessel fuel handling machines (IVHM), as well as the details of the core support structure, are ignored in the mathematical model.

Modeling of the vessel and core barrel are kept as accurate as the code would allow. The flanges, and rings on the vessel and core barrel walls, as well as the thermal liner, are included. They are treated as thin shells of revolution. The inclusion of the core support in the calculation is accomplished by shaping those Lagrangian zones, which represent the core support structure, to conform to the actual configuration. It has the same mass as the actual configuration and is treated as an elastic-plastic solid material. Shields, reflectors, and fission-gas plenum in the mathematical model have the same configuration, mass, compressibility, and wave propagation properties as the actual material. But they are considered to have no tensile strength in the axial and circumferential direction. This will more closely represent the segmented nature of the shields and reflectors which can not resist hoop stresses. The shield plug is modeled as a rigid solid circular plate. It is held down to the ground by holddown bolts. Since holddown bolts constitute a part of the primary boundary, it is felt that some conservatism is needed in the design to prevent the plug from rupture during the slug impact. It is believed that omission of the head deformation would give a somewhat larger impact force on the head cover and thus cause a greater straining of the holddown bolts.

The omission of the instrument trees and the in-vessel fuel handling mechanisms in the mathematical model is based upon the results of the SRI tests [15], which show that a very small amount of energy is deposited in these structures. Since these structures are asymmetric, they can not be faithfully modeled in the two-dimensional analysis, and are therefore excluded in the analysis. Also excluded in the mathematical model are the openings of the inlet and outlet nozzles. This is again the limitation of the two-dimensional analysis.

It is felt that a somewhat conservative approach would be to neglect these openings in the analysis, so that the calculated pressure pulses on the vessel wall are higher.

3.2 Excursion Model

If a small amount of coolant is still in the core during the power excursion, the molten fuel can come into contact with the coolant causing a rapid heating of a relatively small volume of sodium and producing a sodium vapor explosion. Thus, the expansion of the high pressure vapor sodium against the surroundings becomes the mechanism of producing mechanical damage to the system. The sodium expansion model used in the REXCO-HEP analysis is the SOCOOL [17] model which was used to evaluate the mechanical work resulting from the HCDA postulated for the FTR. The mechanical work potential due to the sodium vapor expanding to a pressure of one atmosphere has a magnitude of 150 Mw-sec.

3.3 Discussion of Results

The outputs of the computer code are displacements, velocities, pressures, specific internal energies, densities, strains, stresses, and strain energies. Of extreme importance to the safety analysis is the results of: (1) core barrel deformation, (2) vessel wall deformation, (3) pressure at inlet and outlet nozzles, (4) loads on core support structure, (5) slug impact force, (6) energy portion at slug impact, (7) velocity and displacement of the upper vessel wall, (8) deformation of the holddown bolt system, and (9) ultimate disposition of the excursion energy. The outputs of displacement, velocity and pressure also can be given in graphical form.

As mentioned earlier, the expansion of the high pressure sodium vapor is the mechanism of producing mechanical damage to the system. The sequence of events occurred during the excursion, as follows. As the sodium vapor expands, it first deforms the core surrounding structures (reflectors, shields, etc.). As it expands further, it pushes the core support structure downward, deforms the core barrel and vessel wall radially, and accelerates the liquid sodium above the core upward. The slug of sodium, after being accelerated upward by the expanding core, comes into sudden contact with the reactor cover, and a large impact force is exerted on the head cover and upper vessel wall. The holddown bolts and upper vessel wall are then deformed plastically, thus the energy of the coolant is dissipated in strain energies of the bolts and vessel wall. Finally, the system regains the dynamic equilibrium.

Figure 4 is a series of computer-generated reactor configurations at various times during the excursion. These configurations show how the core surrounding structures are deformed, and how the deformations of the core barrel, vessel wall, and other structures adjacent to the core become progressively larger with time. Figure 4 also shows how the coolant slug is being pushed upward until it comes in contact with the reactor cover and how the upper vessel wall is deformed. The overall flow of the coolant can be followed visually from these configurations.

It is interesting to note that at the time of the slug impact (t = 40.0 msec), the core barrel and the vessel wall at the core region have already deformed to their maximum, but no deformation of the wall at the vessel top has as yet taken place; deformation at the top occurs only after the coolant slug contacts the reactor cover. The maximum deformation of the core barrel is about 6.1%, which occurs at t = 31.91 msec. The maximum deformation of the vessel wall adjacent to the core is about 0.57%. The maximum deformation of the upper

vessel wall resulting from the slug impact with the cover is about 3.5%. Because of the presence of a heavy flange at the top of the vessel wall, the maximum deformation occurs at approximately two zones below the reactor cover. It is also very interesting to note that although the mesh deformation adjacent to the core is significant, the major part of the coolant above the core rises as a unit with very little mesh distortion. The velocity distribution of the coolant body is quite uniform. Because of the presence of the massive core support structure, the downward motion of the coolant is very small, so very little deformation occurs at the lower part of the vessel wall.

It should be mentioned that even with the mesh regularizing scheme in the code, large mesh distortions can still occur in the core region, especially at the core barrel (see Fig. 4e). To overcome this, the distorted zones adjacent to the core barrel have been rezoned. The effect of rezoning can be seen from Figure 4f.

Also of interest is the partition of energy which is shown in Fig. 5 as a function of time. It shows how the core internal energy is transformed into other energies. The work energy released from the core is first transformed into radial and axial kinetic energy of the coolant. Because of the existence of the heavy core support structure, the downward kinetic energy of the coolant is very small. The radial kinetic energy of the coolant is later transformed into strain energy of core barrel and vessel wall (core region). The core barrel strain energy is increasing progressively with time and leveling off after it reaches the dynamic equilibrium. The strain energy of the vessel wall before the slug impact is quite small. After the coolant slug impinged on the reactor cover, the upward axial energy of coolant is transformed into internal energy of coolant, into radial kinetic energy of coolant, and then into strain energy of vessel wall (upper portion) and energy of slug and hold-down bolts. At the time of the incipient slug impact, the work energy released is 67.0 Mw-sec, and the corresponding core vapor pressure is about 24 bars. The partition of the energy released is 66.6% upward kinetic energy, 0.2% downward kinetic energy, 6.3% radial kinetic energy, 17.8% core barrel strain energy, 7.2% vessel strain energy, and 1.9% coolant internal energy.

Since the primary loop is a part of the primary boundary, its containment capability must also be assessed. Pressure pulses at the inlet and outlet nozzles are used as input to the analysis of loads on primary loop components. Figure 6 shows the pressure loading at outlet and inlet nozzle openings obtained from the REXCO-HEP analysis. The maximum pressure at the outlet nozzle from the core sodium vapor expansion is about 50 bars, the maximum pressure at the inlet nozzle is about 30 bars. The lower pressure in the inlet nozzle wall is due to the presence of a heavy massive core support plate that prevented the coolant slug from moving downward. It should be noted that the shape of the two pulses are also different. The peak pressure at the outlet nozzle occurs at a much earlier time than that at the inlet nozzle. This may become an important factor in the evaluation of loads imposed on primary loop components.

The high pressures generated in the hypothetical accident also acts on the core support structure. These loads cause forces to be transmitted up the vessel wall to the vessel support straps. The integrity of the support straps is very important, since the downward acceleration of the reactor vessel is to be arrested by these devices. For this reason, the REXCO-HEP analysis also provides the downward forces on the core support, as shown in Fig. 7. It is very interesting to note that the downward force on the upper surface of the core sup-

port structure, unlike the pressure loading at the nozzle wall openings, has a clearly visible period of oscillation. The time of the period is about 3 msec, which is very close to the natural frequency of the core barrel.

The expansion of the high pressure vapor sodium pushes a coolant slug toward the cover, and upon impact, energy is transferred from the slug to the cover and upper vessel wall. To evaluate the cover stresses and deformations, holddown bolt response, loading on equipment which penetrates or attaches to the vessel head, and effects of missiles, the loading history on the vessel head is needed.

Figure 8 is the cover loading history as obtained from the REXCO-HEP analysis. The slug force consists of a large triangular shape impulse, which lasts for about 2 msec, and a long-duration oscillating residual pressure force. The triangular shape impulse is caused by the sudden contact of the coolant with the cover head. Because the distribution of velocity in the coolant body is not exactly uniform, the peak slug force is smaller than that produced by a uniform-velocity coolant slug, as observed earlier in the REXCO runs [4]. The magnitude of the peak slug force is 85.3×10^{12} dynes, which occurs at t = 42.102 msec. The residual pressure forces following the initial impact are due to the continuous expansion of the core vapor sodium which pushes the coolant slug to further exert pressure on the cover. The total work energy released from the core vapor sodium at t = 92.774 msec is 84.16 Mw-sec, in which 17.16 Mw-sec energy is released after the slug impact.

The distribution of energy at that instant is: (1) upward kinetic energy, 8.11 Mw-sec; (2) downward kinetic energy, 1.32 Mw-sec; (3) radial kinetic energy, 1.31 Mw-sec; (4) core-barrel strain energy, 11.95 Mw-sec; (5) vessel strain energy, 38.11 Mw-sec; (6) coolant internal energy, 7.97 Mw-sec; and (7) energy imparted to reactor head, 15.39 Mw-sec, totaling 84.16 Mw-sec. The gas pressure in the core is about 12-15 bars. The head has moved upward 14.8 cm; the axial velocity of the head at that instant is 111 cm/sec. The 15.39 Mw-sec energy imparted to the reactor head can be further partitioned into: (1) kinetic energy of head, 0.39 Mw-sec; (2) potential energy of head, 0.89 Mw-sec; and (3) holddown bolt strain energy 14.11 Mw-sec, totaling 15.39 Mw-sec.

The primary containment system is already in dynamic equilibrium at t = 92.774 msec. The unreleased HCDA work energy will be retained in the core for a relatively long period of time if the sodium is not allowed to spill out of the primary containment. This is also true for the sodium kinetic energy. The sodium will be in vibratory motion for a long time until it is finally damped out by the viscous frictional force. The additional energy imparted to the reactor head and vessel wall will be very small.

From the results of the REXCO-HEP analysis, it can be concluded that the reactor vessel will remain intact in the 150 Mw-sec HCDA and the postaccident heat can be continuously removed from the damaged core. A large safety margin is also provided in the holddown bolt design and the cover will not become a missile.

4. Conclusions

It has been demonstrated that REXCO-HEP has the capability of predicting accurately the response of the primary containment to an HCDA and to give guidance as to the effects of such an accident in a fast reactor system.

The ultimate intent of the analytical effect in developing the REXCO series of codes is to produce dependable calculational tools, fully verified by experiments, that can predict

the hydrodynamic and structural response to HCDAs, not only in FTR, but also in future LMFBRs. Considerable progress has been made in this area. There have been satisfactory comparisons with experiment work performed in Europe, with the NOL experiment and the SL-1 accident, and more recently with the SRI simple and complex scale experiments in support of the FTR.

It is recognized that the answer one obtains from the computer analysis depends upon the basic information and the mathematical model used in the computer analysis. To improve computer results, a better understanding of the energy release mechanisms and more reliable equation-of-state data for the core materials, the fission gas and the sodium coolant over the appropriate pressure and temperature ranges are needed. Also needed are the dynamic properties of the reactor structural materials under very rapid loading and proper modeling of complicated structures such as the core support structure and the reactor cover.

Once the information described above becomes available, the designer will have more confidence in REXCO and similar containment computer codes. It is believed that extensive explosive testing programs will not be necessary to assess the containment capability of reactor systems. Future tests may be needed only for rather unusual reactor or primary system configurations. Also, understanding of the behavior of individual internal components and their effects on the primary system may require testing so that appropriate mathematical models can be formulated for these components.

References

[1] FISTEDIS, S. H., "Containment of Fast Breeder Reactors - Present Status - Remaining Problems," First Intl. Conf. on Structural Mechanics in Reactor Technology, Berlin, Germany, September 20-24, 1971.

[2] CHANG, Y. W., GVILDYS, J., FISTEDIS, S. H., "Hydrodynamic Response of Primary Reactor Containment to High-energy Excursion," Nucl. Eng. Design 12, 344-360 (1970).

[3] CHANG, Y. W., GVILDYS, J., FISTEDIS, S. H., "Two-dimensional Hydrodynamics Analysis for Primary Containment," ANL-7498 (November, 1969).

[4] CHANG, Y. W., GVILDYS, J., "Dynamic Response of Reactor Containment to High-energy Excursion," Proc. the First Intl. Conf. on Structural Mechanics in Reactor Technology, Berlin, Germany, (September 20-24, 1971).

[5] VON NEUMANN, J., RICHTMYER, R. D., "A Method of the Numerical Calculation of Hydrodynamic Shocks," J. Appl. Physics 21, (3), pp. 232-237 (1950).

[6] BUTLER, T. D., "LINC Method Extensions," Second Intl. Conf. on Numerical Methods in Fluid Dynamics, Berkeley, California, September 15-19, 1970.

[7] WILKINS, M. L., "Calculation of Elastic-plastic Flow," UCRL-7322, Rev. 1 (January, 1969).

[8] MAENCHEN, G., SACK, S., "The Tensor Code," UCRL-7316 (April, 1963).

[9] HOSKIN, N. E., SLOUGH, M. R., "Stabilization of Mesh Distortion in the 2-D Lagrangian Code ASTARTE," UKAEA GRO/44/91/16.

[10] ASH, J. E., JULKE, R. T., "Comparison of a Two-dimensional Hydrodynamics Code (REXCO) to Excursion Experiments for Fast Reactor Containment," ANL-7911, (January, 1972).

[11] ASH, J. E., CHANG, Y. W., JULKE, R. T., "Comparison of a Two-dimensional Hydrodynamics Code (REXCO) to Excursion Experiments for Fast Reactor Containment, ANL-7911, Suppl. 1 (July, 1972).

[12] Reactor Development Progress Report, ANL-RDP-8, p. 9.54 (August, 1972).

[13] Reactor Development Progress Report, ANL-RDP-14, p. 9.54 (February, 1973).

[14] DENISE, R. P., et al, "Containment of Fast Breeder Reactors - Recent Developments in Analytical and Experimental Methods," The Intl. Conf. on Engineering of Fast Reactors for Safe and Reliable Operations, Karlsruhe, Germany, Oct. 9-13, 1972.

[15] FLORENCE, A. L., Abrahamson, G. R., "Simulation of a Hypothetical Core Disruptive Accident in a Fast Flux Test Facility," SRI Report (to be published).

[16] NAGUMO, G., "Validation of an Explosive Energy Source for use in Scaled Model Tests with a Two-dimensional Hydrodynamics Code (REXCO)." ANL Topical report (to be published).

[17] PADILLA, A., "Transient Analysis of Fuel-sodium Interactions," Trans. Amer. Nucl. Soc., 13, p. 375 (1970).

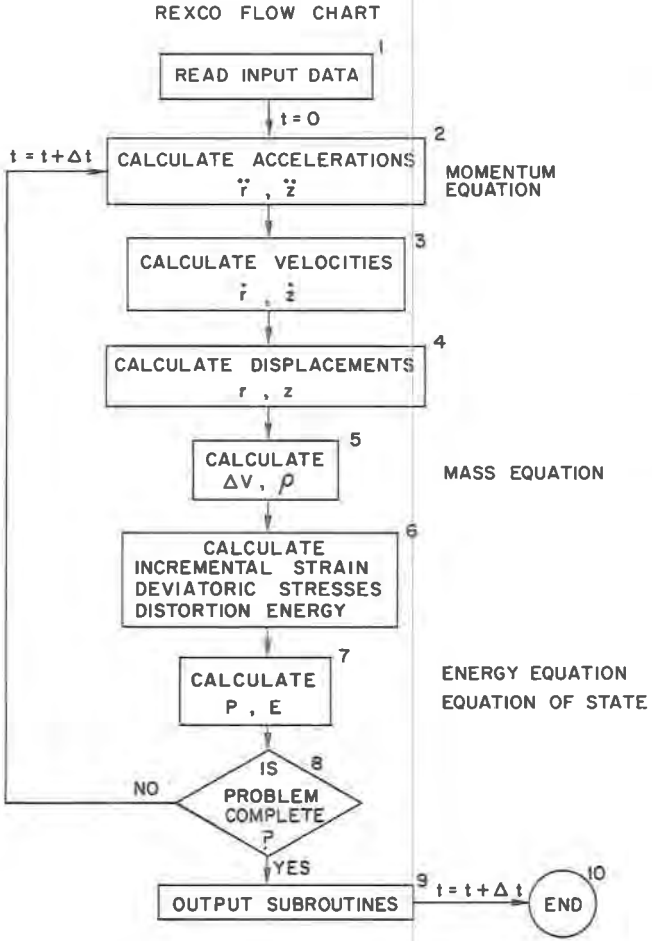

(1) REXCO Flow Chart.

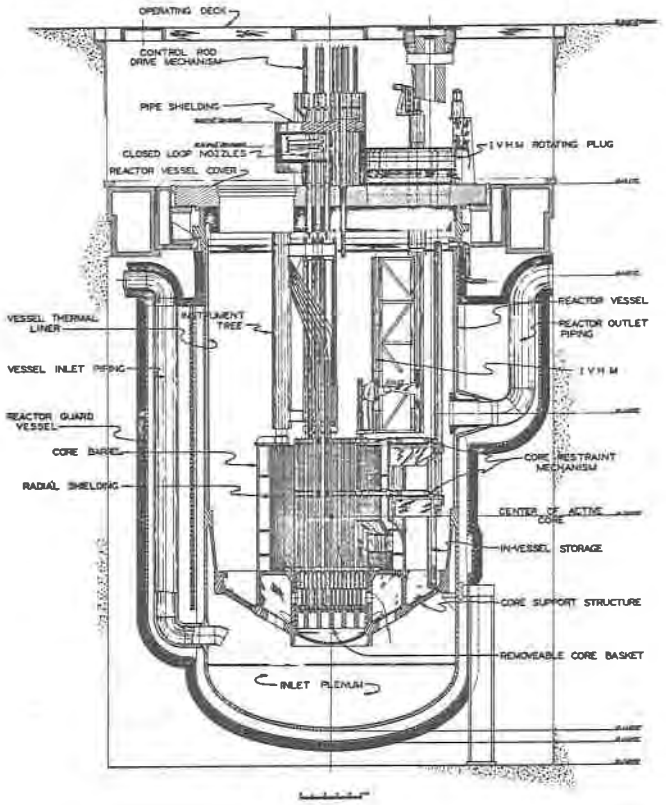

(2) FTR Reactor Configuration.

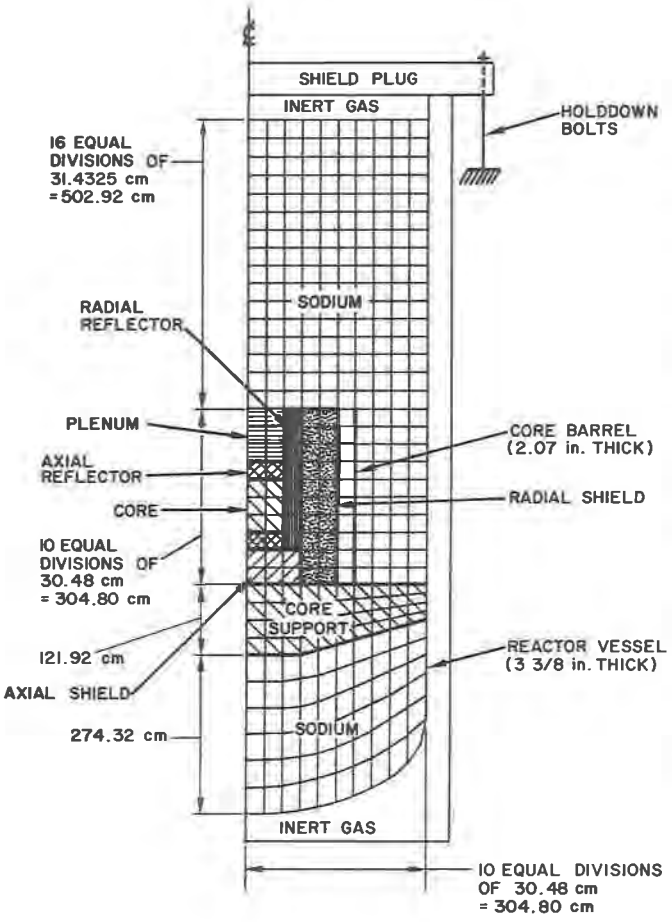

(3) REXCO Mathematical Model for HCDA Analysis.

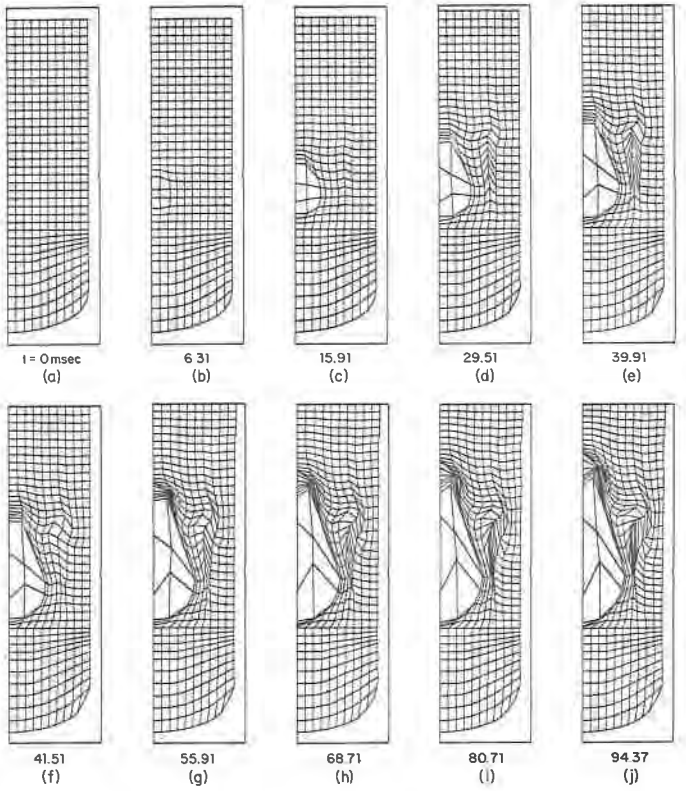

(4) Reactor Configurations at Various Times during Excursion.

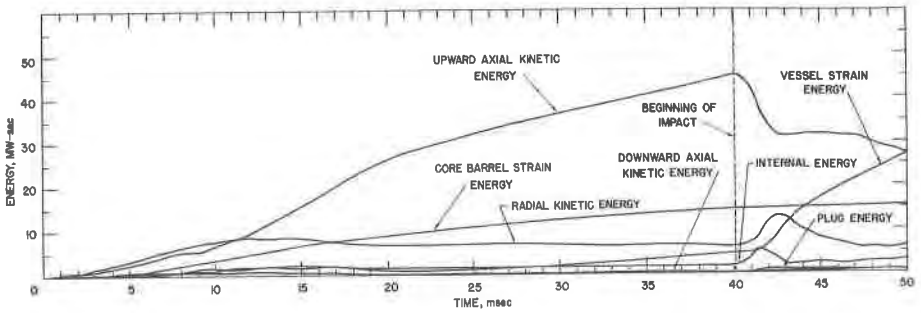

(5) Energy Partition.

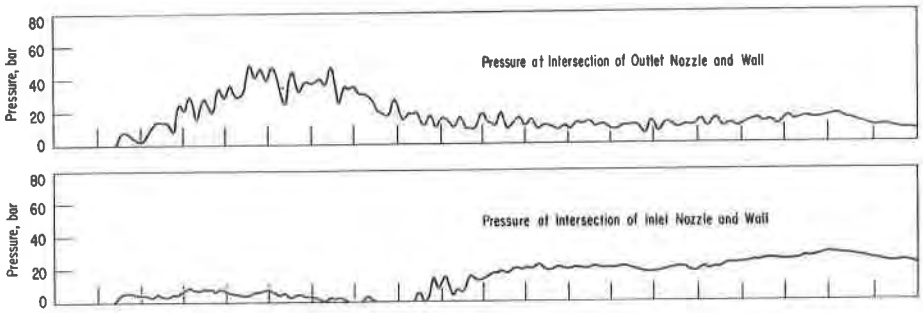

(6) Pressures at Nozzles.

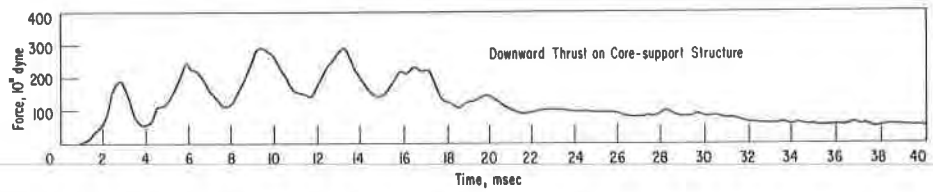

(7) Downward Thrust on Core-support Structure.

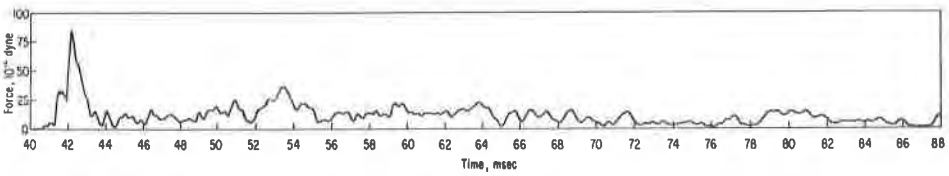

(8) Slug-impact Force.